Journal of Hazardous Materials 178 (2010) 377–384

Contents lists available at ScienceDirect

Journal of Hazardous Materials

journal homepage: www.elsevier.com/locate/jhazmat

Role of dissolved organic matters (DOM) in membrane fouling of membrane bioreactors for municipal wastewater treatment

Shujuan Tang, Zhiwei Wang*, Zhichao Wu, Qi Zhou

State Key Laboratory of Pollution Control and Resource Reuse, Key Laboratory of Yangtze River Water, Environment of Ministry of Education, School of Environmental Science and Engineering, Tongji University, 1239 Siping Road, Shanghai 200092, PR China

ARTICLE INFO

Article history:
Received 6 July 2009
Received in revised form 15 January 2010
Accepted 16 January 2010
Available online 25 January 2010

Keywords:
Dissolved organic matter (DOM)
DOM fraction
Membrane bioreactor (MBR)
Membrane fouling
Wastewater treatment

ABSTRACT

Two membrane bioreactors (MBRs) with different operation conditions were employed to investigate the role of dissolved organic matter (DOM) in membrane fouling. DOM characteristics and their correlations with membrane fouling in the MBR systems were studied by using three-dimensional excitation-emission matrix (EEM) fluorescence technology, gel filtration chromatography (GFC) analysis, and column chromatographic method for DOM fractionation, etc. The three-dimensional EEM fluorescence spectroscopy analysis indicated that the fluorescence intensity of protein-like peaks in DOM samples collected from the MBR zones showed positive correlations with membrane fouling. The fluorescence spectra of membrane foulants also exhibited two protein-like peaks, confirming that proteins played an important role in membrane fouling. The DOM samples collected from MBR zones were fractionated into four components, i.e., hydrophobic (HPO), transphilic (TPI), charged hydrophilic (HPI-C) and neutral hydrophilic fractions (HPI-N). It was found that HPI-N was the most abundant fraction in all the samples, accounting for 42.0–48.9% of the total DOM. Test results also showed that HPI-N had the highest fouling potential, which could be attributed to the high molecular weight (MW) distribution and the high membrane rejection rate of macromolecules.

1. Introduction

Membrane bioreactor (MBR) has been used for decades in wastewater treatment and reclamation as a modification of the conventional activated sludge (CAS) process, which separates the effluent and activated sludge by filtration instead of sedimentation. MBR process offers the extra advantages over conventional treatment technology such as a smaller footprint, less sludge production, better effluent quality, etc. [1–3]. However, membrane fouling remains the primary obstacle limiting the widespread application of MBRs [4,5].

Dissolved organic matter (DOM) is ubiquitous in surface water and sewage, and have been a major concern in water and wastewater treatment systems. DOM was widely reported to be the main cause of membrane fouling in drinking water treatment by microfiltration (MF) and ultrafiltration (UF) of surface waters [6–9]. In biological wastewater treatment, DOM, of which the majority is soluble microbial products (SMP), affects both the kinetic activity and flocculating properties of activated sludge [4]. Along with the increase of MBR applications in wastewater treatment, the influence of dissolved organic fractions in mixed liquors on MBR performance has attracted more attention recently [3,10,11]. Since the concentration of sludge in MBR systems is several magnitude orders higher than DOM, it was considered to be a key factor influencing membrane fouling [12,13]. However, the relative contribution of DOM to membrane fouling has been reported in the range of 26–52% [2,14,15]. DOM originated from biological wastewater treatment process may include organic compounds of different groups, such as carbohydrates, proteins and more biologically resistant components known as fulvic and humic acid materials [16,17]. Several researchers have reported that polysaccharide-like substances contributed to fouling more significantly than protein-like substances [11,18], while Hernandez Rojas et al. [19] found that the concentration of proteins in SMP showed significant influences on membrane fouling in terms of the specific resistances increase. With a smaller molecular weight (MW), humic acid substances contained in the liquid phase could not be retained by the membrane, and therefore may not significantly participate in MBR fouling [20]. However, the importance of humic acid substances to membrane fouling has also been reported recently. Liang and Song [3] found that aquatic humic acid substances were the major component of DOM responsible for membrane fouling in MBRs. Those controversial reports make it hard to understand the DOM characteristics, in particular the characteristics of fractional DOM components. Researches on the correlations of DOM fractions with membrane fouling have been carried out in drinking water treatment [6,7];

* Corresponding author. Tel.: +86 21 65980400; fax: +86 21 65980400.
E-mail address: zwwang@tongji.edu.cn (Z. Wang).

0304-3894/$ – see front matter © 2010 Elsevier B.V. All rights reserved.
doi:10.1016/j.jhazmat.2010.01.090

however, the information about the influence of fractional DOM on membrane fouling in MBRs for wastewater treatment is still limited. Therefore, it is very essential to study the different roles that the various DOM fractions play in MBR fouling and to achieve a better understanding of DOM properties in MBRs.

The purpose of this study is, therefore, to obtain more detailed characteristics of DOM and their corresponding role in membrane fouling in MBR systems. DOM samples collected from MBRs under different operating conditions were characterized by three-dimensional excitation-emission matrix (EEM) fluorescence spectroscopy and gel filtration chromatography (GFC). In particular, DOM samples were fractionated into four components on the basis of hydrophobic/hydrophilic property and charge by column chromatographic method, and the characteristics of the each fractional DOM component were further examined and analyzed.

2. Materials and methods

2.1. Experimental setup and operation conditions

Two identical pilot-scale MBRs each with an effective volume of 58.6 L were used in this study (Fig. 1). Each MBR consisted of four zones, i.e., anaerobic zone (8.0 L), anoxic zone (15.3 L), alterable zone (7.3 L) and MBR zone (28.0 L). The MBR zone was installed with two 0.2 μm polyvinylidene fluoride (PVDF) flat-sheet membrane modules (SHZZ-MF, Zizheng Environmental Inc., Shanghai, China). The effective filtration area of each module was 0.175 m^2. Aeration was provided at the bottom of the MBR zone in order to supply oxygen for microorganisms and to induce a cross-flow velocity along membrane surfaces for membrane fouling control. The dissolved oxygen (DO) concentration in the MBR zone and other zones were kept in the range of 1–3 mg/L and <0.2 mg/L, respectively. An aeration diffuser together with a stirrer was located at the alterable zone to achieve different operation modes. The first operation mode could be obtained by turning off the aeration and switching on the stirrer of the alterable zone, and the second operation mode was achieved when the aeration on and the stirrer off. Mixed liquors of the MBR zone and the alterable zone were recycled to the anoxic zone (recirculation I) and the anaerobic zone (recirculation II), respectively. Different operation runs were obtained by changing the sludge retention time (SRT), hydraulic retention time (HRT), aeration mode and recycle rate. The detailed operating conditions of the four runs are summarized in Table 1. A temperature controller was set in the MBR in Run 2 to provide a constant operation temperature of 20 ± 2 °C, while other runs were operated under temperature seasonal change. A pump was used to withdraw the effluents through the membrane at a filtration-to-idle ratio of 8 min/2 min. The MBRs were operated under constant flux mode, and the trans-membrane pressure (TMP) was monitored with a pressure gauge. Chemical cleaning-in-place procedure (0.5% (v/v) NaClO solution, 2 h duration) would be carried out if the TMP reached about 30 kPa during the operation. The influent to the experimental setup was municipal wastewater, and the characteristics of the wastewater are as follows: COD 297.6 ± 113.0 mg/L, TN 48.9 ± 10.4 mg/L, NH_3–N 30.8 ± 8.4 mg/L and TP 5.32 ± 1.4 mg/L (number of measurements: n = 39).

Table 1
Operation conditions of four MBR runs.

Run	1	2	3	4
SRT (d)	60	60	60	40
HRT (h)	10.2	10.2	8.2	10.2
Rate of recirculation I	3	3	2	2
Rate of recirculation II	1	1	0.5	0.5
[a]Aeration mode	1	1	2	1
Temperature in MBR phase (°C)	7.3–26.1	18.2–22	9.4–23.8	9.5–23.8
MLSS in MBR phase (g/L)	3.7–7.6	4.5–5.9	7.3–11.0	4.5–8.1

[a] 1 and 2 means that the alterable zone was operated under the first operation mode and the second operation mode, respectively.

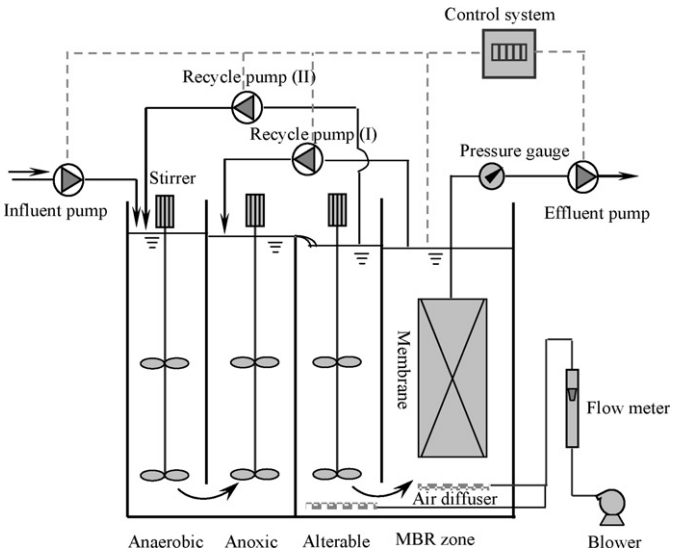

Fig. 1. Flow diagram of the MBR setup.

2.2. Collection and pre-treatment of membrane foulants

The fouled membrane modules were taken out from the bioreactor at the end of each operation cycle when the TMP reached about 30 kPa. The gel layer on the membrane surfaces was carefully scraped off by a plastic sheet and simultaneously flushed with deionized (DI) water. The collected sample was placed on a magnetic blender (Model JB-2, Leici Instrument Inc., Shanghai, China) and well mixed. The DOM sample of membrane foulants was obtained by filtering the mixed liquor through a 0.45 μm polyethersulfone (PES) membrane filter (Gelman Supor 450, Pall Corporation, USA).

2.3. DOM fractionation method

DOM samples of the influent wastewater and the mixed liquors of MBR zones were obtained by filtering those samples through a 0.45 μm PES membrane filter (Gelman Supor 450, Pall Corporation, USA). The effluent water was also filtered through the PES membrane filter to obtain the effluent DOM. The fractionation procedure was carried out according to the method described by Park et al. [21] and Dong et al. [6]. All the DOM samples were adjusted to pH 2, and adsorbed by DAX-8 (Supelco Company, PA, USA) and XAD-4 resins (Amberlite, Rohm & Hass Company, PA, USA) sequentially. The hydrophobic (HPO) and transphilic (TPI) fractions were obtained by eluting the DAX-8 and XAD-4 resins with 0.1 M NaOH solution, respectively. The effluent of XAD-4 was adjusted to pH 8 and fed onto Amberlite IRA-958 resin (Amberlite, Rohm & Hass Company, PA, USA), which retained the charged hydrophilic (HPI-C) fraction. This fraction was eluted with a NaOH/NaCl mixture. The remaining neutral hydrophilic (HPI-N) fraction was not adsorbed by any of the resins.

2.4. Fouling potential test

Fouling potential was measured with a dead-end filtration apparatus as described by Shen et al. [22]. The DOC concentration of the fractionated components was adjusted to 5 mg/L with milli-Q water (Milli-Q Gradient, MILLIPORE, USA) and the pH was adjusted

to 7 with hydrochloric acid and NaOH solution before the fouling potential tests. The membrane employed in the fouling potential tests was the same as the membrane used in the MBR runs. Each of the new membrane was soaked in DI water for 24 h and further cleaned through filtering 300 mL DI water to remove any impurities prior to measuring the fouling potential of the samples. The TMP was kept at 30 kPa by a vacuum pump during the test. Filtration resistance caused by DOM (R_f) was calculated according to Eq. (1).

$$R_t = R_f + R_m \quad (1)$$

where R_t is total membrane resistance (m^{-1}), R_m intrinsic resistance of the new membrane (m^{-1}). R_f and R_m were calculated by the following equation:

$$J = \frac{TMP}{\mu R} \quad (2)$$

where μ is the permeate water viscosity (Pa s), J the membrane flux ($m^3/(m^2\,h)$) and R the filtration resistance (m^{-1}).

The filtrated volume and filtration time were recorded in order to calculate J according to Eq. (3). R_m and R_t were obtained by filtrating DI water and the DOM samples, respectively.

$$J = \frac{\Delta V}{A\Delta t} \quad (3)$$

where ΔV is the filtration volume (m^3), Δt the filtration time (s) and A the membrane area (m^2).

2.5. Analytical methods

Measurements of chemical oxygen demand (COD), total nitrogen (TN), total phosphorus (TP) and ammonia (NH_3–N) in the influents and membrane effluents, mixed liquor suspended solids (MLSS) in the system were performed according to the Chinese NEPA standard methods [23]. The DO concentration in the reactor was measured by a dissolved oxygen meter (Model YSI 58, YSI Research Inc., OH, USA). The dissolved organic carbon (DOC) was analyzed by a total organic carbon (TOC) analyzer (LiquiTOC trace, ELEMENTAR, Germany). Carbohydrate concentration was measured according to the phenol–sulfuric acid method [24] with glucose as the standard reference, whereas the modified Lowry method [25] was used for protein determination with bovine serum albumin (BSA) as the standard reference.

The three-dimensional EEM fluorescence spectra were measured using a luminescence spectrometry (F-4500 FL spectrophotometer, HITACHI, Japan). The EEM spectra were collected with the scanning emission spectra from 200 nm to 500 nm at 5 nm increments by varying the excitation wavelengths from 200 nm to 400 nm at 5 nm sampling intervals. The excitation and emission slits were maintained at 10 nm and the scanning speed was set at 1200 nm/min for this study. The EEM spectra are plotted as the elliptical shape of contours. The X-axis represents the emission spectra while the Y-axis indicates the excitation wavelength, and the third dimension, i.e., the contour line, is shown to express the fluorescence intensity at an interval of 5.

The MW distribution of the DOM samples were measured by GFC analyzer, which consisted of a TSK G4000SW type gel column (TOSOH Corporation, Japan) and a liquid chromatography spectrometer (LC-10ATVP, SHIMADZU, Japan). Polyethylene glycols (PEGs) (CAS number: 25322-68-32, Merck Chemicals Inc., Germany) were used as standards for calibration. The elution at different time intervals was collected by an automatic fraction collector and automatically analyzed by using a UV spectroscope and a dissolved organic carbon (DOC) analyzer to obtain a MW distribution curve.

Table 2
Effluent water characteristics of MBR runs (mg/L)[a].

Run	COD	TN	NH_3–N	TP
1	21.5 ± 9.0	13.3 ± 5.0	0.93 ± 2.30	2.2 ± 0.3
2	23.8 ± 6.6	11.3 ± 3.8	0.90 ± 1.23	3.1 ± 0.9
3	22.1 ± 16.4	14.2 ± 4.3	0.54 ± 1.7	2.3 ± 1.1
4	22.4 ± 34.2 (10–56)	11.1 ± 6.4	0.78 ± 1.6	2.0 ± 1.1

[a] Values are given as mean value ± standard deviation; number of measurements: n = 15 (Run 1 and run 2), n = 24 (Run 3 and Run 4).

3. Results and discussion

3.1. MBR process performance

Table 2 summarizes the average effluent water characteristics of the four runs. It can be seen that the removal of COD, TN and NH_3–N was quite successful in all the four runs, and the TP was reduced by 42–59%. It should be noted that Run 1 and Run 2 were operated under the same conditions except temperature. The average temperature in MBR zone of Run 1 was only 11.9 °C while it was kept at 20 ± 2 °C in Run 2 by using a temperature controller. The effluent TN concentration of Run 2 was lower than that of Run 1, which confirmed that temperature influenced the removal efficiency of nitrogen. It was reported that nitrification activity could be depressed under low temperature operation in the nitrogen removal process [26]. However, effluent NH_3–N was not varied significantly under low temperature in our study, while higher concentration of nitrate of Run 1 was detected compared to Run 2, indicating that the restriction step of the nitrogen removal was denitrification at low temperature. The TP removal was not obviously improved either by the temperature increase in Run 2 or the decrease of SRT in Run 4, which might be due to the fact that the SRT of 40 d was still too long for biological removal of TP.

The variations of TMP during the MBR runs are shown in Fig. 2. The fouling rate was determined by the TMP increase rate per unit time. In order to compare the overall fouling behaviour of the four runs, the TMP increase rate in a run was averaged among all the cycles during the experiment. The order of fouling rate was

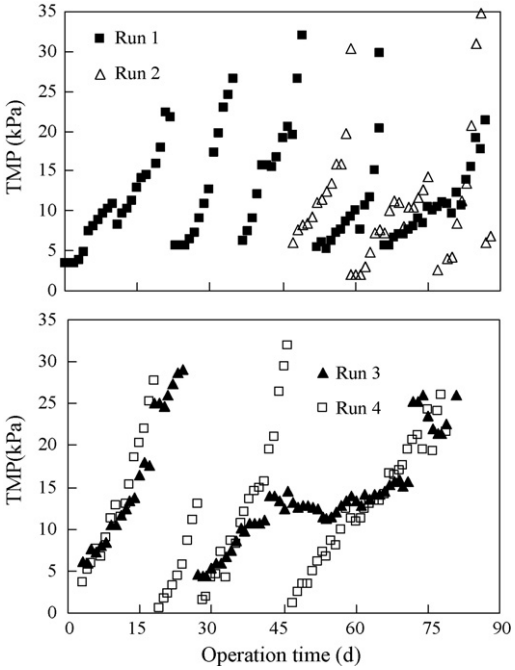

Fig. 2. Variations of TMP during the experiments.

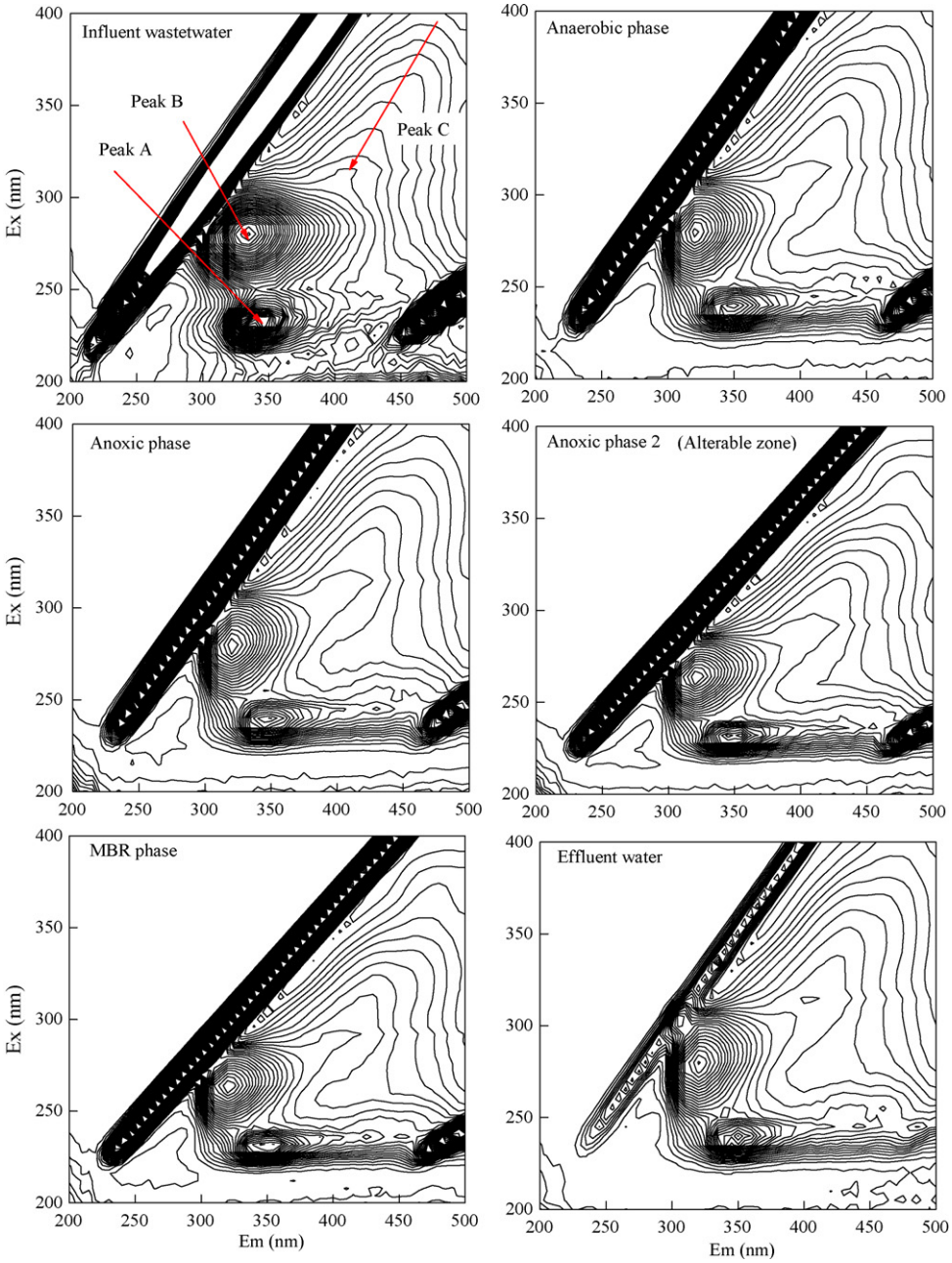

Fig. 3. Variations of EEM fluorescence spectra of DOM in MBR process (Run 1).

Run 3 (0.77 kPa/d) < Run 4 (1.40 kPa/d) < Run 1 (1.46 kPa/d) < Run 2 (2.13 kPa/d). Run 3 demonstrated best filtration performance while membrane fouling occurred most rapidly in Run 2 even though it was operated under higher temperature. This could be owing to the different DOM characteristics under different operation conditions, which will be discussed in detail in the following sections. It is worth noting that temperature did have an influence on TMP variations and thus membrane fouling rate. The temperature also affected the DOM variations. In this study, we operated the MBRs at various temperature and operational conditions in order to observe the correlations between variation of TMP and the variation of DOM. The variation of temperature between runs was designed by us, i.e., Run 2 was controlled by a temperature controller, and other runs were operated naturally (the seasonal temperature change will induce the temperature variations in the MBR). Other factors might also influence the membrane fouling rate, e.g., the various MLSS concentration. The difference of the MLSS concentration in the four runs could also contribute the difference of DOM in the four runs. It is also reported that DOM plays an important role in membrane fouling of MBRs under sub-critical flux operation compared to MLSS [3,4].

3.2. Three-dimensional EEM fluorescence spectroscopy

The typical three-dimensional EEM fluorescence spectra of DOM samples during the treatment process in Run 1 are illustrated in Fig. 3, including DOM of the anaerobic, anoxic, alterable and MBR zone together with the influent and effluent DOM (similar EEM spectra were obtained in other three runs and not shown here). Two main fluorescence peaks could be identified from the EEM fluorescence spectra of all the DOM samples. Peak A was detected at the excitation/emission wavelengths (E_x/E_m) of 235–240/340–355 nm,

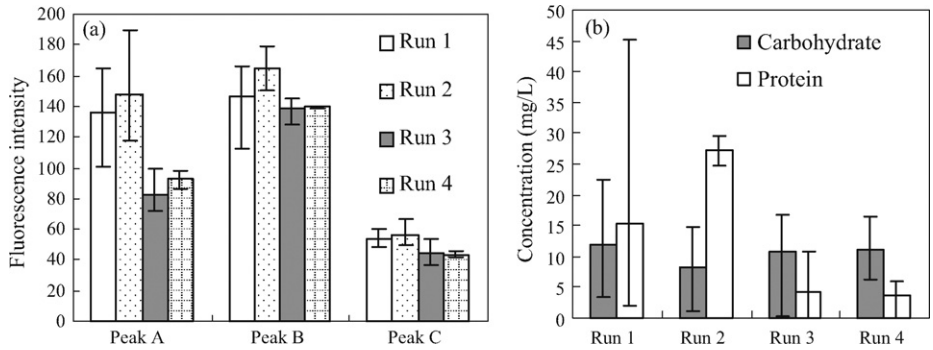

Fig. 4. (a) Fluorescence intensity of DOM MBR phase of different runs ($n = 2$) and (b) concentration of carbohydrate and protein in DOM ($n = 6$).

while Peak B was located at the E_x/E_m of 280–285/320–335 nm. The two peaks have been ascribed to protein-like substances in which the fluorescence was associated with the tyrosine (Peak A) and tryptophan (Peak B), respectively [27,28]. A minor peak (Peak C) with E_x/E_m at 310–315/400–420 nm was also observed for most of the samples. This peak has been reported to be associated with humic acid-like substances [28,29].

Contour lines in the spectra are illustrated to indicate the fluorescence intensity, and thicker contour lines indicate higher fluorescence intensity. The fluorescence intensity of Peak A and B in DOM of the anaerobic zone was much lower than that of the influent DOM, while the changes were not significant from the anaerobic zone to the MBR zone. The fluorescence intensity of Peak A and Peak B was reduced slightly after membrane filtration, suggesting that the membrane could retain, to some extent, protein-like substances. However, the intensity of Peak C, related to humic acid-like substances with low biodegradability, was stable in the treatment process.

Location of the peak was another parameter indicating the characteristics of the DOM. The location of Peak A was gradually red-shifted by 5–10 nm during the treatment process. Compared to the influent DOM, Peak B of DOM in the anaerobic zone was blue-shifted by 15 nm along the excitation axis, while no change of the location was observed in DOM of the subsequent biological treatment zones and the effluent DOM. A slight red shift along emission axis of Peak C was also observed. A red shift is related to the presence of carbonyl-containing substituents, hydroxyl, alkoxyl, amino groups and carboxyl constituents [29,30], while a blue shift is associated with decomposition of condensed aromatic moieties and the break-up of the large molecules into smaller fragments, such as a decrease in the number of aromatic rings, a reduction of conjugated bonds in a chain structure, a conversion of a linear ring system to a non-linear system or an elimination of particular functional groups including carbonyl, hydroxyl and amine [31,32]. The shifts of Peak A and Peak B locations indicated that besides the concentration, the structure of protein-like substances also changed in the MBR systems. The protein-like substances in the influent wastewater, which might exist as large aromatic molecules, were degraded into small molecules, corresponding to the blue shift of Peak A and the red shift of Peak B.

The fluorescence intensity of three peaks of DOM in the MBR zone of the four runs was compared (Fig. 4(a)). It could be observed that the fluorescence intensity of Peak A and Peak B was positively related to the membrane fouling rate, i.e., Run 3 (0.77 kPa/d) < Run 4 (1.40 kPa/d) < Run 1 (1.46 kPa/d) < Run 2 (2.13 kPa/d). It indicated that protein-like substances in DOM played an important role in membrane fouling. The fluorescence intensity of Peak C, which was much lower than that of Peak A and Peak B, also had a similar trend with the fouling rate, suggesting that humic acid-like substances also contributed to membrane fouling. It should be pointed out that other factors, e.g., MLSS, temperature, etc., could also influence the membrane fouling rate. As discussed earlier, the DOM may play a more important role in MBRs under sub-critical flux operation compared to MLSS [3,12]. The fluorescent intensity of peaks in DOM obtained in our study could indicate the membrane fouling behaviour in MBRs, which also supported that the DOM had significant correlations with membrane fouling.

Many reports considered that carbohydrates were a more important factor causing membrane fouling than protein and humic acid-like substances [11,18]. Herzberg et al. also reported that the carbohydrates induced more severe fouling of reverse osmosis (RO) membranes compared to proteins [33]. However, the concentration of carbohydrates determined by the phenol–sulfuric acid method [24], as shown in Fig. 4(b), had no obvious correlations with fouling rate (Run 3 < Run 4 < Run 1 < Run 2) in this study. The concentration of proteins in four runs correlated to fluorescence intensity and membrane fouling rate except the relationship between Run 3 and Run 4. The differences between our study and other researchers' reports could be due to the various influent wastewater and membrane materials employed during the experiments. Other operational parameters could also exert influences on DOM characteristics, e.g., shear stress was found to induce the increase of proteins in an MBR but without obvious influences on carbohydrates in the mixed liquor [34]. The modification of membranes could also vary the contribution of proteins to membrane fouling and was beneficial to control membrane fouling of proteins and other polymeric substances [35].

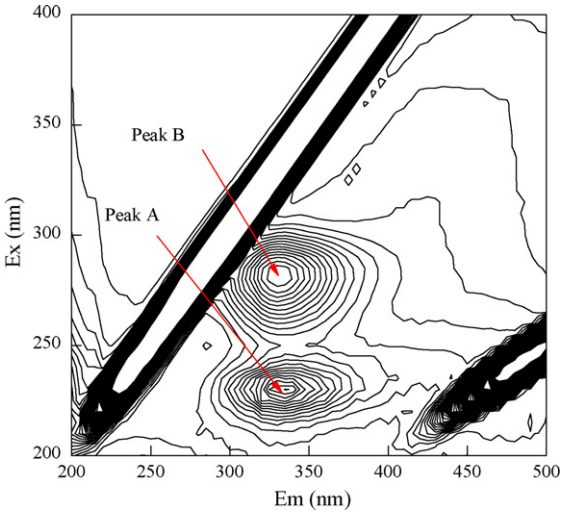

Fig. 5. EEM fluorescence spectra of dissolved membrane foulants.

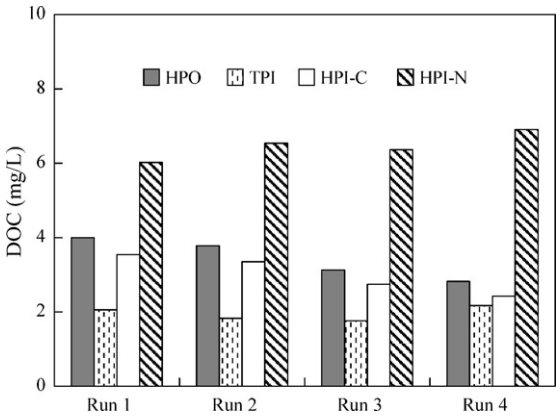

Fig. 6. Fractional components of DOM in MBR phase of different runs.

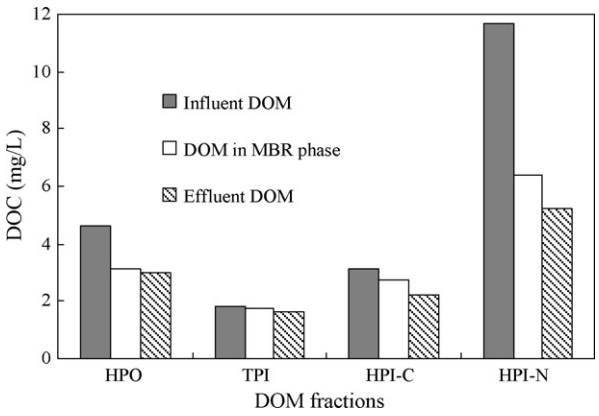

Fig. 8. Variations of DOM fractions in MBR systems.

The EEM fluorescence spectra of dissolved membrane foulants in Run 1 are shown in Fig. 5 (similar EEM profiles of membrane foulants were obtained in other three runs and not shown here). Compared to the fluorescence spectra of DOM in the MBR zone, Peak A exhibited a blue shift by 10–15 nm and Peak B was red-shifted along emission axis by 10 nm, indicating that the protein structure of DOM in foulants was different from that of the DOM in the MBR zone. Peak C was found to be almost neglected in the membrane foulants, implying that humic acid-like substances caused membrane fouling mainly by adsorbing into membrane pores (pore blocking) rather than by accumulating onto the membrane surface to form a fouling layer.

3.3. DOM fractionation

The concentrations of DOM fractions, in terms of DOC, are shown in Fig. 6. For all the DOM samples collected from MBR zones in the four runs, HPI-N component was found to be the most abundant fraction, accounting for 42.0–48.9% of the total DOM. The HPO fraction was the second largest portion, accounting for 19.7–24.2%, which was less than the reported results of 43.8–65.7% in MBR systems treating synthetic municipal wastewater [3]. This could be attributed to the different wastewater used in our study (real municipal wastewater) and their study (synthetic wastewater).

More detailed research was carried out in order to obtain a better understanding of the characteristics of each DOM fraction, including the fouling potential of fractional components (Fig. 7(a)) and MW distribution (Fig. 7(b)). The order of the fractional component fouling potential in terms of increase of filtration resistance was found to be HPI-N > HPO > TPI > HPI-C. The fractional component HPI-N in DOM had strongest fouling potential in the MBRs, which is in good agreement with the findings that were obtained in microfiltration of natural organic matter (NOM) in surface waters [36]. HPO component, predominantly humic acids, was reported as a major fouling factor in membrane filtration systems for surface water treatment as well [7,8]. In our study, HPO fraction also demonstrated significant fouling propensity in the MBR systems. It could be observed that HPI-N component had higher content of much larger MW organic molecules compared with other fractional components. MW of the HPI-N component mostly (about 99%) distributed in the range of over 10,000 Da, while the most of HPI-C had a MW lower than 1000 Da. The MW of HPO fraction was a little larger than that of TPI fraction, and the two components had the most abundant MW distribution between 1000 and 10,000 Da. The high fouling potential of HPI-N fraction could be attributed to large MW and the neutral characteristics that made it easy to foul and adsorb on membrane surfaces [36]. The MW of HPO and TPI fraction was found to be larger than that of HPI-C component in the MBR systems in our study, and these findings are consistent with the reported research on NOM fractional components in surface water treatment [9,37]. HPO and TPI fractions, which had larger MW distribution compared to HPI-C, demonstrated higher fouling potential than HPI-C (see Fig. 7(a)).

It has been reported that the rejection or retention of organic matter by membranes plays an important role in membrane fouling in ultrafiltration process for surface water treatment [37]. In order to better understand DOM rejection characteristics and related fouling mechanisms in MBR systems, the variations of fractional DOM concentration during the treatment process were analyzed and shown in Fig. 8. It could be observed that fractional DOM was reduced gradually from the influent DOM to DOM in MBR phase to the effluent DOM in the MBR systems, which indicated

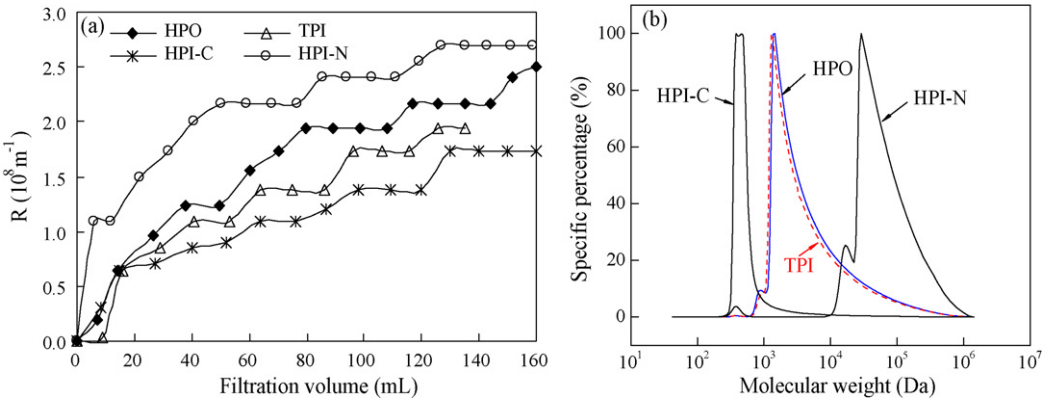

Fig. 7. (a) Filtration resistance variations of DOM fractions and (b) MW distribution curves of DOM fractional components.

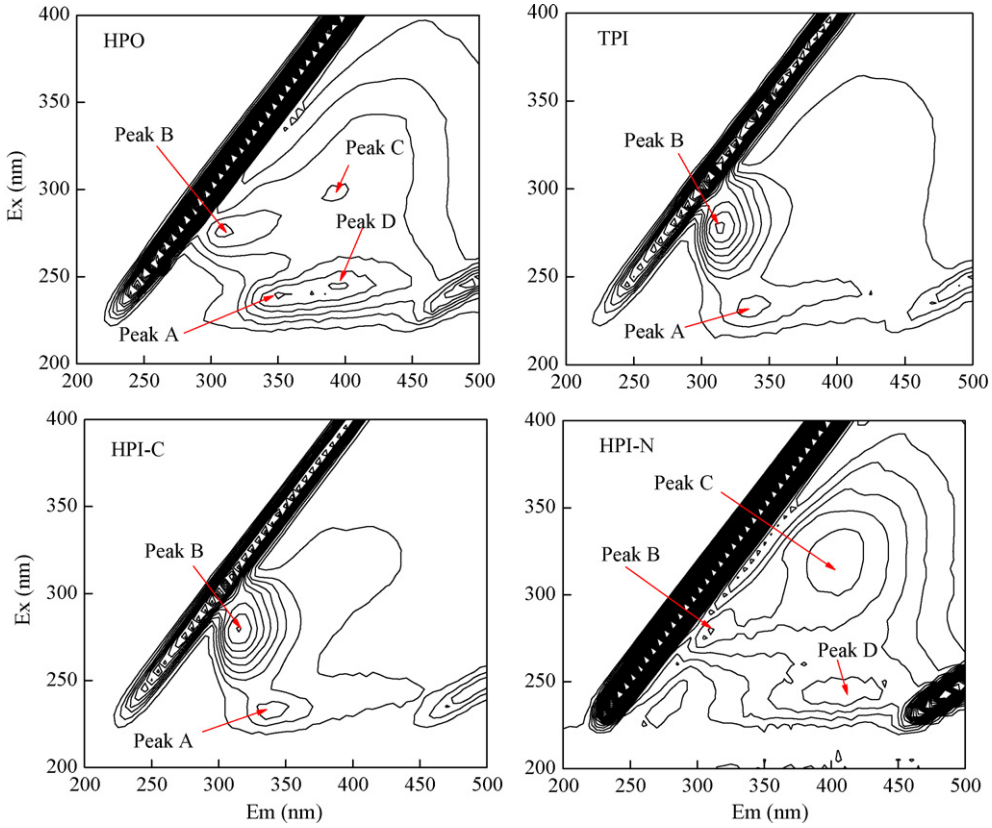

Fig. 9. EEM fluorescence spectra of different DOM fractions.

that the fractional DOM was firstly degraded by microorganisms and then rejected by fine pores of membranes. The HPI-N fraction with a reduction rate of 45.5% showed the highest biodegradability among the DOM fractions, followed by HPO (reduction rate 32.3%), HPI-C and TPI. Membrane rejection of HPI-N was also more remarkable compared with other fractions, which was mainly due to HPI-N's high MW distribution. It is worth noting that although the membrane rejection rate of HPI-C was higher than HPO and TPI fractions, the HPI-C fraction had the lowest fouling potential (see Fig. 7(a)). This might be attributed to the charge repulsion between the charged DOM and the charged fouling layer formed on membrane surfaces, which needs further investigating.

EEM fluorescence spectra (Fig. 9) of fractional DOM were analyzed in our study in order to clarify the compounds present in the various DOM fractions. A fluorescence peak (Peak D), which was reported to be associated with fulvic acid-like substances [29], was detected at the E_x/E_m of 245/400–435 nm in the HPO and HPI-N fractions. Aromatic protein-like substances (Peak A), tryptophan protein-like substances (Peak B), humic acid-like substances (Peak C) and fulvic acid-like substances (Peak D) were present in HPO fraction, while there was a lack of Peak A in the EEM spectra of HPI-N fraction. Only two main peaks (Peak A and Peak B) were observed in the EEM spectra of TPI and HPI-C fractions, and fluorescence intensity of Peak B was larger than that of Peak A, suggesting that tryptophan protein-like substances were dominant in the two fractions compared with aromatic protein-like substances. The interactions among a mixture of the various compound types and combined effects of the compounds in HPO and HPI-N fractions might explain why the two fractions had higher fouling potential than TPI and HPI-C fractions, which is consistent with the research carried out by Gray et al. [38] in the microfiltration process for surface water treatment.

4. Conclusions

DOM characteristics and their role in membrane fouling in MBR systems were studied by using three-dimensional EEM fluorescence technology, GFC analysis, and column chromatographic method for DOM fractionation, etc. Based on this study, the following conclusions could be drawn.

(1) Three obvious fluorescence peaks were detected in the DOM of the MBR systems. Two main peaks were associated with protein-like substance and the third was attributed to humic acid-like substance. The fluorescence intensity of Peak A and Peak B was reduced by the biological treatment and membrane rejection, while Peak C was relatively stable in the process.
(2) The fluorescence intensity of protein-like peaks in DOM collected from MBR zones of four runs was found to be positively related to the membrane fouling rate. The protein concentration measured by traditional methods confirmed the important role of protein in membrane fouling, while the concentration of carbohydrate showed no obvious trend with membrane fouling rate. Moreover, Peak A and Peak B were also detected in fluorescence spectra of membrane foulants, indicating protein-like substance accumulated on the membrane surfaces to induce membrane fouling.
(3) DOM samples were fractionated into four components, i.e., HPO, TPI, HPI-C and HPI-N, on the basis of hydrophobicity/hydrophilicity and charge. HPI-N and HPO components were found to have higher fouling potential than the other two fractions. HPI-N, which was the most abundant fraction in all the samples, showed the largest MW distribution and fouling rate. Meanwhile, HPI-N showed the highest biodegradability and membrane rejection rate, which correlated with its high fouling potential.

Acknowledgements

Financial support of this work by the Key Special Program on the S&T for the Pollution Control and Treatment of Water Bodies (Grant No. 2008ZX07316-002 and 2008ZX07101-003) and by the Independent Research Fund of Chinese Stake Key Laboratory of Pollution Control and Resource Reuse for Young Scholars (Grant No. PCRRY08005) is gratefully acknowledged.

References

[1] H.P. Chu, X.Y. Li, Membrane fouling in a membrane bioreactor (MBR): sludge cake formation and fouling characteristics, Biotechnol. Bioeng. 90 (2005) 323–331.
[2] W. Lee, S. Kang, H. Shin, Sludge characteristics and their contribution to microfiltration in submerged membrane bioreactors, J. Membr. Sci. 216 (2003) 217–227.
[3] S. Liang, L. Song, Characteristics and fouling behaviours of dissolved organic matter in submerged membrane bioreactor systems, Environ. Eng. Sci. 24 (2007) 652–662.
[4] D.J. Barker, D.C. Stuckey, A review of soluble microbial products (SMP) in wastewater treatment systems, Water Res. 33 (1999) 3063–3082.
[5] Z. Wang, Z. Wu, S. Tang, Extracellular polymeric substances (EPS) properties and their effects on membrane fouling in a submerged membrane bioreactor, Water Res. 43 (2009) 2504–2512.
[6] B. Dong, Y. Chen, N. Gao, J. Fan, Effect of coagulation pre-treatment on the fouling of ultrafiltration membrane, J. Environ. Sci. 19 (2007) 278–283.
[7] H.C. Kim, J.H. Hong, S. Lee, Fouling of microfiltration membranes by natural organic matter after coagulation treatment: a comparison of different initial mixing conditions, J. Membr. Sci. 283 (2006) 266–272.
[8] W. Yuan, A. Zydney, Humic acid fouling during microfiltration, J. Membr. Sci. 157 (1999) 1–12.
[9] A.W. Zularisam, A.F. Ismail, M.R. Salim, M. Sakinah, O. Hiroaki, Fabrication, fouling and foulant analyses of asymmetric polysulfone (PSF) ultrafiltration membrane fouled with natural organic matter (NOM) source waters, J. Membr. Sci. 299 (2007) 97–113.
[10] P. Paul, C. Hartung, Modeling of biological fouling propensity by inference in a side stream membrane bioreactor, Desalination 224 (2008) 154–159.
[11] S. Rosenberger, H. Evenblij, S. Poele, T. Wintgens, C. Laabs, The importance of liquid phase analyses to understand fouling in membrane assisted activated sludge processes–six case studies of different European research groups, J. Membr. Sci. 263 (2005) 113–126.
[12] L. Defrance, M.Y. Jaffrin, B. Gupta, P. Paullier, V. Geaugey, Contribution of various constituents of activated sludge to membrane bioreactor fouling, Bioresour. Technol. 73 (2000) 105–112.
[13] Y. Magara, M. Itoh, The effect of operational factors on solid/liquid separation by ultramembrane filtration in a biological denitrification system for collected human excreta treatment plants, Water Sci. Technol. 23 (1991) 1583–1590.
[14] E.H. Bouhabila, R.B. Aim, H. Buisson, Fouling characterization in membrane bioreactors, Sep. Purif. Technol. 22–23 (2001) 123–132.
[15] C. Wisniewski, A. Grasmick, Floc size distribution in a membrane bioreactor and consequences for membrane fouling, Colloid Surf. A: Physicochem. Eng. Aspects 138 (1998) 403–411.
[16] T. Ilani, E. Schulz, B. Chefetz, Interactions of organic compounds with wastewater dissolved organic matter: role of hydrophobic fractions, J. Environ. Qual. 34 (2005) 552–562.
[17] A. Imai, T. Fukushima, K. Matsushige, Y.H. Kim, K. Choi, Characterization of dissolved organic matter in effluents from wastewater treatment plants, Water Res. 36 (2002) 859–870.
[18] N.O. Yigit, I. Harman, G. Civelekoglu, H. Koseoglu, N. Cicek, M. Kitis, Membrane fouling in a pilot-scale submerged membrane bioreactor operated under various conditions, Desalination 231 (2008) 124–132.
[19] M.E. Hernandez Rojas, R. Van Kaam, S. Schetrite, C. Albasi, Role and variations of supernatant compounds in submerged membrane bioreactor fouling, Desalination 179 (2005) 95–107.
[20] A. Drews, M. Vocks, V. Iversen, B. Lesjean, M. Kraume, Influence of unsteady membrane bioreactor operation on EPS formation and filtration resistance, in: Proceedings of the International Congress on Membranes and Membrane Processes (ICOM), Seoul, Korea, 2005.
[21] C. Park, H. Kim, S. Hong, S. Choi, Variation and prediction of membrane fouling index under various feed water characteristics, J. Membr. Sci. 284 (2006) 248–254.
[22] H. Shen, X.Q. Cui, Q.T. Jin, H.Y. Hu, Comparison of filtration characteristics of sludges from aerobic and anaerobic MBRs, Membr. Technol. 27 (2007) 27–31.
[23] Chinese NEPA, Water and Wastewater Monitoring Methods, third ed., Chinese Environmental Science Publishing House, Beijing, China, 1997.
[24] M. Dubois, K.A. Gilles, J.K. Hamilton, P.A. Rebers, F. Smith, Colorimetric method for determination of sugars and related substances, Anal. Chem. 28 (1956) 350–356.
[25] E.F. Hartree, Determination of protein: a modification of the Lowry method that gives linear photometric response, Anal. Biochem. 48 (1972) 422–427.
[26] D.J. Kim, D.I. Lee, J. Keller, Effect of temperature and free ammonia on nitrification and nitrite accumulation in landfill leachate and analysis of its nitrifying bacterial community by FISH, Bioresour. Technol. 97 (2006) 459–468.
[27] N. Maiea, N.M. Scully, O. Pisani, R. Jaffé, Composition of a protein-like fluorophore of dissolved organic matter in coastal wetland and estuarine ecosystems, Water Res. 41 (2007) 563–570.
[28] Z. Wang, Z. Wu, S. Tang, Characterization of dissolved organic matter in a submerged membrane bioreactor by using three-dimensional excitation and emission matrix fluorescence spectroscopy, Water Res. 43 (2009) 1533–1540.
[29] W. Chen, P. Westerhoff, J.A. Leenheer, K. Booksh, Fluorescence excitation–emission matrix regional integration to quantify spectra for dissolved organic matter, Environ. Sci. Technol. 37 (2003) 5701–5710.
[30] J. Świetlik, A. Dabrowska, U. Raczyk-Stanislawiak, J. Nawrocki, Reactivity of natural organic matter fractions with chlorine dioxide and ozone, Water Res. 38 (2004) 547–558.
[31] P.G. Coble, Characterization of marine and terrestrial DOM in seawater using excitation-emission matrix spectroscopy, Mar. Chem. 51 (1996) 325–346.
[32] J. Świetlik, E. Sikorska, Application of fluorescence spectroscopy in the studies of natural organic matter fractions reactivity with chlorine dioxide and ozone, Water Res. 38 (2004) 3791–3799.
[33] M. Herzberg, S. Kang, M. Elimelech, Role of extracellular polymeric substances (EPS) in biofouling of reverse osmosis membranes, Environ. Sci. Technol. 43 (2009) 4393–4398.
[34] A. Menniti, S. Kang, M. Elimelech, E. Morgenroth, Influence of shear on the production of extracellular polymeric substances in membrane bioreactors, Water Res. 43 (2009) 4305–4315.
[35] A. Asatekin, A. Menniti, S. Kang, M. Elimelech, E. Morgenroth, A.M. Mayes, Antifouling nanofiltration membranes for membrane bioreactors from self-assembling graft copolymers, J. Membr. Sci. 285 (2006) 81–89.
[36] L. Fan, J.L. Harris, F.A. Roddick, N.A. Booker, Influence of the characteristics of natural organic matter on the fouling of microfiltration membranes, Water Res. 35 (2001) 4455–4463.
[37] J. Cho, G. Amy, J. Pellegrino, Membrane filtration of natural organic matter: factors and mechanisms affecting rejection and flux decline with charged ultrafiltration (UF) membrane, J. Membr. Sci. 164 (2000) 89–110.
[38] S.R. Gray, C.B. Ritchie, T. Tran, B.A. Bolto, Effect of NOM characteristics and membrane type on microfiltration performance, Water Res. 41 (2007) 3833–3841.